Original Paper

Energy Evolution Characteristics of Coal–Rock Composite Bodies Based on Unidirectional Load

Xuanhong Du [1,2] **Junhua Xue,**[1] **Qian Ma,**[1] **Zhiheng Chen,**[1] **and Keliang Zhan**[1]

Taking coal mine dynamic disaster as research background in this paper, five samples of coal–rock composite bodies (CRCBs) with different coal thicknesses were designed, and the uniaxial loading tests were carried out on them by using the MTS uniaxial loading instrument and the DS5 acoustic emission instrument, and the damage process of the samples were analyzed from the perspective of energy conversion. The results were as follows. With increase in coal thickness of CRCBs, the uniaxial compressive strength and elastic modulus of CRCBs decreased while the peak strain increased, and the overall bearing capacity of the samples decreased, resulting in a decreasing trend of AE peak ringing count and peak energy. According to the theory of conservation of energy, it was found that the dissipated energy of the samples in the compaction stage accounted for a large proportion, and the elastic stage was dominated by the accumulation of elastic energy. After the plastic stage, the energy conversion rate in the samples accelerated, and the dissipated energy increased rapidly, leading to the gradual failure of the samples. The energy storage limit of samples decreased logarithmically together with increase in coal thickness. Finally, it was found that coal was the main energy storage structure of the whole coal and rock composite system by analyzing the energy accumulation mechanism of coal and rock composite structure in practical engineering. Therefore, to prevent and control underground dynamic disaster in practical engineering, the internal energy storage of a coal seam should be released and the clamping effect of roof and floor on coal body should be weakened. The achievements of this study will be a theoretical guidance for preventing and controlling dynamics.

INTRODUCTION

Large-scale underground engineering, such as mining engineering, tunnel engineering and underground construction engineering, are affected by some dynamic disasters to some degrees during the construction period, seriously affecting the smooth progress of a project (Li et al., 2020, 2021a, 2021b; Shi et al., 2021, 2022; Zhao et al., 2022). With increase in mining depth, the in-situ stress increases rapidly. The in-situ stress concentration caused by mining leads to catastrophic accidents, such as rockburst, seriously threatening the lives of mineworkers, and brings new challenges to safe mining of deep coal seams (Yang et al., 2020, 2021a, b; Liu et al., 2020a, 2021a, b; Li et al., 2021a, b; Chen et al., 2021; Maleki, 2021; Pang et al., 2021; Yang & Zhang, 2021). Rockbursts have been a cosmopolitan problem for years, and it has occurred in China, Russia, South Africa, Germany, Britain, and other

[1]College of Safety Science and Engineering, Xi'an University of Science and Technology, Xi'an 710054, Shaanxi, China.
[2]To whom correspondence should be addressed; e-mail: 15349419043@163.com

countries (Mroz & Nawrocki, 1989; Pan et al., 2003; Wang, 2021; Yu et al., 2021a, b). Researchers have never stopped studying it, and various mechanisms and related theories of rockburst have been proposed, as shown in Table 1 (Wang & Huang, 2012). According to energy theory, the damage and failure essence of coal rock is an instability phenomenon driven by transmission and conversion of energy (Zhang et al., 2019; Ma et al., 2021; Sun et al., 2021). Under the action of continuous energy dissipation and release, the bearing capacity of coal and rock gradually decreases until it is destroyed, leading to the occurrence of high-energy-level engineering disasters (Liu et al., 2021a, b; Xu et al., 2021; Zhang et al., 2021). However, many factors, such as mine occurrence condition, stress distribution characteristics, and coal rock status, all affect the occurrence of high-energy-level underground engineering disasters, and mining of a coal seam will inevitably destroy roof and floor. Therefore, it is necessary to treat coal seam, roof and floor as conflated to study energy conversion characteristics of coal–rock composite bodies (CRCBs).

Over the years, many scholars have studied the occurrence mechanism of high-energy-level mine disasters in the process of coal mining through a variety of research methods, such as theoretical analysis, numerical simulation, and experiment analysis, which have made important contributions to the prevention and control of high-energy-level disasters in coal mines. It was found that the deformation and failure of coal rock mass under a complex stress state always showed a nonlinear characteristic. In order to describe this phenomenon accurately, many scholars have established a coal body damage model to facilitate the study of nonlinear constitutive relationships of coal bodies, which can be used as reference and basis for future research (Lemaitre, 1984; Li & Zhang, 2017; Cao et al., 2017; Chen et al., 2018a, 2018b; Liu & Dai, 2018; Wang et al., 2018; Yin et al., 2018; Liu & Liu, 2021). With the continuous complement of theory and mechanism, the damage and failure constitutive model of rock mass is modified frequently, providing an important theoretical support for the establishment and modification of numerical model. In addition, the change situation of the stress field induced by secondary excavation is difficult to monitor accurately by existing technical means due to the complexity of mining engineering and tunnel engineering. Therefore, numerical simulation is used widely in the simulation of high-energy-level disas-

ters during the construction of coal mining engineering, tunnel engineering, and other projects (Zhu et al., 2017; Chen et al., 2018a, 2018b; Jiang et al., 2018; Niu, 2018; Wang et al., 2019a, 2019b; Yang et al., 2019; Zhang et al., 2020). In fact, under the action of concentrated stress, coal and rock mass always accumulate energy and release energy in different forms during the coal seam and tunnel excavation, so as to achieve the state of energy balance. However, it is difficult to study the characteristics of failure and energy of coal and rock mass directly in the field site. Therefore, scholars usually select small samples as the breakthrough points to study the failure behavior and energy characteristics of coal and rock mass.

Huang and Liu (2013) carried out uniaxial compression tests of composed coal rock at different loading rates, the effect of the rate and path of loading and unloading on the mechanical properties of the composed coal rock has been analyzed. Zhao et al. (2017) studied the influence of bedding angle and loading rate on the fractures initiation and propagation of coal. Meng et al. (2018) studied the influences of loading and unloading mode on the characteristics of energy accumulation and energy dissipation during rock deformation and failure, and the evolution and distribution laws of energy accumulation and dissipation in the rock during the pre-peak stage were revealed. Chen et al. (2019) conducted uniaxial and triaxial compression tests on mudstone, proposed damage coefficient, and analyzed rock mechanical properties and damage evolution process from the perspective of energy. Zhou et al. (2019) tested the mechanical properties of sandstone under triaxial cyclic loading, the concepts of elastic energy conversion rate and elastic energy conversion function were proposed to discuss the principles of energy evolution of rocks under triaxial cyclic loading tests. He et al. (2021) made coal–rock combined samples to study their mechanical behaviors and energy characteristics. In the experiment process, the AE equipment is often used to monitor the failure behavior of the samples. High-precision AE equipment can locate accurately the initial position and propagation evolution of fractures within the samples under the condition of loading, as well as monitor AE events and AE energy in the process of specimen failure stage (Schiavi et al., 2011; Li et al., 2021; Lu et al., 2021; Miao et al., 2021; Xue et al., 2021a, 2021b), providing important reference for analyzing the failure behaviors and failure degree of samples.

Table 1. Related theories of rockburst

Theory	Typical representative	Content
Strength theory	Brauner (1975)	Answer why material is damaged; but in practice, rockburst may not occur when coal (rock) is damaged, and rockburst is related to the sudden failure of coal and rock mass
Energy theory	(Cook, 1963, 1965; Salamon, 1964a, 1964b, 1964c)	The energy theory solves the problem of where energy comes from when rockburst occurs. However, the energy theory does not answer why energy is released in a sudden release instead of dissipation in a slow manner
Stiffness theory	(Cook et al., 1966; Deist, 1965)	The ideological core of stiffness theory is still theoretical
Deformation instability theory	(Qi et al., 1997; Zhang, 1987; Zubelewica & Mroz, 1983)	The theory of deformation instability explains rockbursts from the viewpoint of break mechanics, and initially answers the problem of sudden destruction of coal. However, the physical mechanism of material breakage is still not clear

The occurrence of high-energy-level disasters, such as rockburst, is not only related to rock mass but also to coal. Many previous studies focused on some kind of rock or coal, and few of the research selected CRCBs as research object. In the study of CRCBs, the rock part of CRCBs is usually selected for rocks with certain properties rather than sampling from roof or floor rocks. However, coal seams and rock strata in different regions are affected by different degrees of crustal movement, geological deposition and weathering and corrosion, and so the occurrence conditions of coal seams are obviously different. After a coal seam is excavated, the front coal and its roof and floor will be affected to some degrees, and the energy stored in them will be released. High-energy-level dynamic disasters, such as rockburst, are caused by the sudden release of a large amount of energy accumulated in a coal–rock system under the action of mine pressure. Therefore, it is necessary to treat coal seam, roof and floor as conflated to study the energy conversion characteristics of CRCBs, and provide support for the study of high-energy-level dynamic disasters from the perspective of energy conversion.

EXPERIMENTAL PROGRAM

Sample Preparation

To ensure the uniformity of both the occurrence conditions of samples and the development degree of initial fractures, samples were selected from a coal seam, roof, and floor in the same roadway of a mine in Henan Province. The samples were wrapped with plastic and then put in wooden boxes filled with sawdust to prevent the samples from being deformed and damaged by external forces during transportation.

The samples were processed according to the relevant provisions of methods for determining the physical and mechanical properties of coal and rock. First, cylindrical samples with diameter of 50 mm were drilled using a coring drill, then the coal samples were sawed into 10, 20, 30, 40, and 50 mm-high cylinders using a stone sawing machine, and the rock samples were sawed into 25, 30, 35, 40, and 45 mm-high cylinders. Finally, both ends of the coal sample and the rock sample were ground and polished with a grinding machine. The non-parallelism of both ends of the samples was required to be < 0.01 mm, the deviation of diameter was < 0.02 mm. The prepared samples were wrapped with plastic and put into a curing box for curing.

Test Equipment

The loading device was MTS uniaxial compression testing machine. The displacement control mode was selected to carry out the test, and the loading rate was 0.001 mm/s. The AE parameter acquisition device was DS5 AE instrument. The test process is shown in Figure 1.

Principle of Acoustic Emission Test

Under the action of external force, the stress concentration phenomenon will occur in the initial fracture region within a sample, and the microfractures will generate and propagate continuously inside the sample (Zhao et al., 2020; Hong et al., 2021). In addition, strain energy will accumulate in
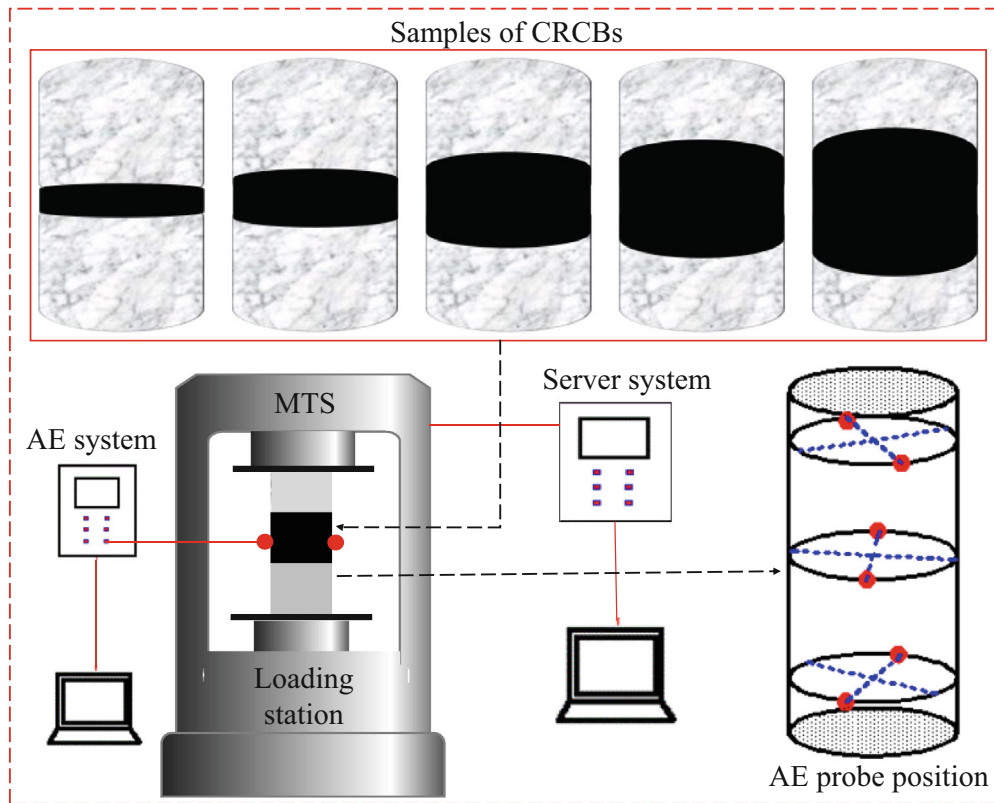
Figure 1. Test material and equipment schematic.

this process, and the release form of strain energy is the elastic wave. The essential of damage and failure is the result of energy dissipation and release. The energy dissipation results in reduction in mechanical properties and load-bearing capacity of a sample. Energy release leads directly to the overall failure of a sample, and so energy is an important parameter to measure the deformation and failure of a sample (Dong et al., 2021; Zhou & Zhang, 2021). The schematic diagram of AE test principle is shown in Figure 2.

EXPERIMENTAL RESULT

Analysis of Stress–Strain Curve of CRCBs

Through uniaxial compression test, the variation relationship between load (P) and deformation (ΔL) during the loading process was obtained. The test data were processed according to the following equations:

$$\sigma_i = \frac{P_i}{A} \tag{1}$$

$$\varepsilon_i = \frac{\Delta L_i}{L} \tag{2}$$

where σ_1 is the stress (MPa) on the sample at a certain time, P_i is the load (kN) corresponding to σ_1, ε_i is the strain corresponding to P_i, ΔL_i is the deformation (m) corresponding to ε_i, L is the axial length (m) of CRCBs, and A is the cross-sectional area (m^2) of the CRCBs. Then, the stress–strain curves of the CRCBs with different coal thicknesses were obtained (Fig. 3).

The uniaxial compressive strengths of CRCBs with coal thickness of 10, 20, and 30 mm were 22.08, 19.89, and 18.59 MPa, respectively. During the loading process of these three samples of CRCBs, the middle coal part of the CRCBs first generated damage fractures under the action of external forces. Then, under the continuous action of axial stress, the failure deformation of CRCBs resulted in fractures
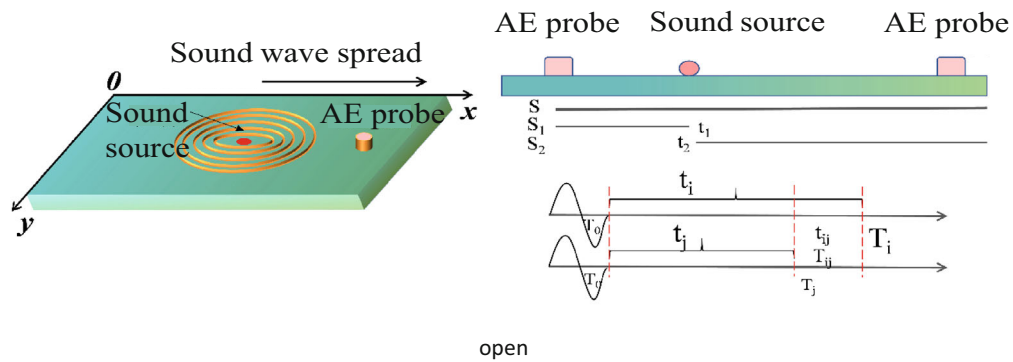
open

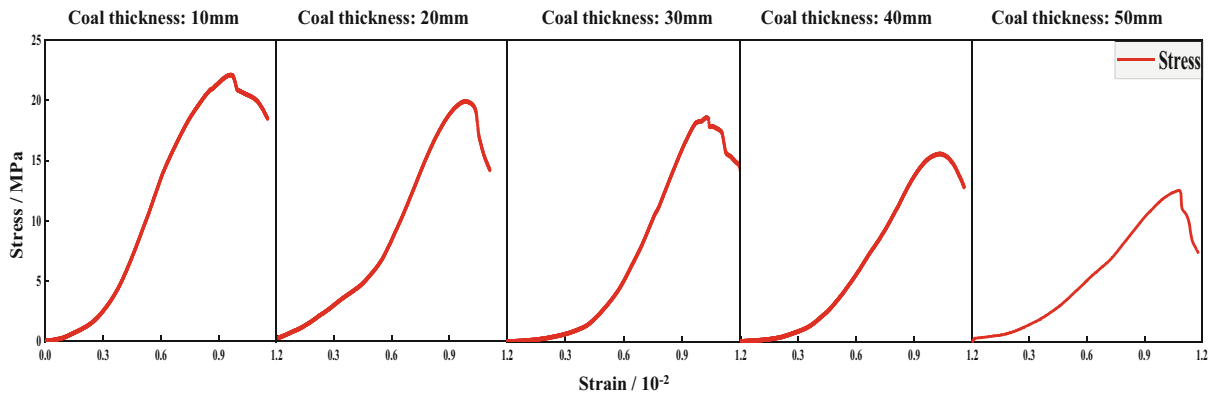**Figure 2.** Schematic diagram of the test principle of acoustic emission.

Figure 3. Stress–strain curves of samples of CRCBs.

generation in the upper and bottom rock mass until failure. The overall strengths of the three samples of CRCBs depended on the rock part due to the small proportion of coal part.

The uniaxial compressive strengths of CRCBs with coal thickness of 40 and 50 mm were 15.61 and 12.57 MPa, respectively. The uniaxial compressive strengths of the two samples of CRCBs decreased significantly. This is because the proportion of coal part of these two samples of CRCBs exceeded that of rock part. During the test, the rock parts of CRCBs were not damaged significantly after the middle coal part was broken in a large area and lost its bearing capacity. Therefore, the overall strengths of the two samples of CRCBs depended on the coal part.

Parameters, such as uniaxial compressive strength, elastic modulus, and peak strain of CRCBs have a great influence on the energy variation characteristics of CRCBs. The variations of uniaxial compressive strength, elastic modulus, and peak strain of the CRCBs with different coal thicknesses are shown in Figure 4.

It is seen from the Figure 4 that the uniaxial compressive strength and elastic modulus of the CRCBs decreased linearly with increase in coal thickness, while the peak strain showed a linear increasing trend. This is because the coal part of the CRCBs had experienced a long period of sedimentary metamorphism, and it is under the condition of high depth and high stress, which resulted in the generation of more internal micro-fractures and pores compared to the roof and floor rock part, and with increase in coal thickness of the CRCBs the initial fractures of the CRCBs increased. Because the bearing capacity of the middle coal part was weaker than that of the rock part of CRCBs, the overall bearing capacity of the CRCBs decreased,
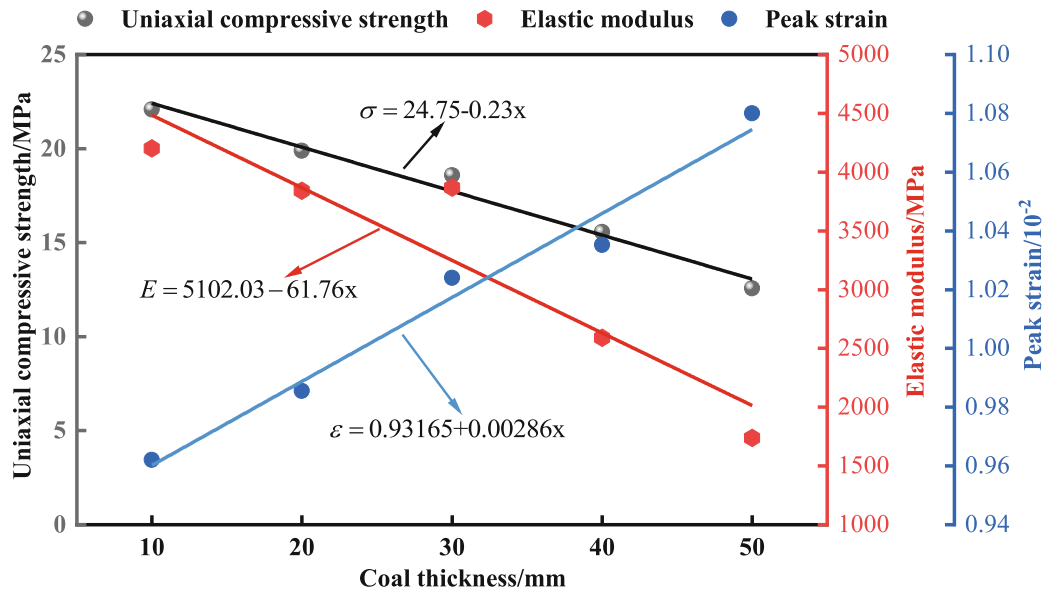
Figure 4. Variations of uniaxial compressive strength, elastic modulus, and peak strain of the CRCBs with different coal thicknesses.

which led to the decrease in uniaxial compressive strength, elastic modulus. With increase in coal thickness of the CRCBs, the brittleness decreased and the ductility increased, resulting in the increase in peak strain (Yu et al., 2021a, 2021b).

Acoustic Emission Characteristics of CRCBs

During the test, the continuous axial stress caused the deformation and failure of the CRCBs, and the samples experienced the process of accumulation and release of strain energy. In the test, the elastic energy released in the failure process of the sample was captured by the AE signal monitoring equipment, so as to analyze the failure characteristics of the CRCBs. The variation characteristics of the AE parameters of the CRCBs are shown in Figure 5.

It is seen from Figure 5 that the ringing counts and energy at different stress stages of the CRCBs showed good correspondence, and the characteristics of each stage are distinct. The change relationship between AE ring counts and energy is closely related to the failure process of the CRCBs. According to the trend of AE parameters in Figure 5, the variation characteristics of AE events in the failure process of the CRCBs were classified into three stages: (1) stable development stage, (2) active stage, and (3) drastic development stage.

The stable development stage of AE event occurred mainly in the fracture compaction stage and elastic stage of the stress–strain curve. At the initial stage of loading, the initial fractures and defects in the CRCBs began to close gradually under the action of axial stress, and the AE ring counts and energy were lower. After entering the elastic stage, micro-fractures generated in some areas of the CRCBs and propagated gradually under the action of axial stress, the CRCBs experienced a recoverable elastic deformation, and the AE ring counts and energy increased.

The active stage of AE event occurred mainly in the plastic stage of stress–strain curve. The generation rate of micro-fractures in the CRCBs increased rapidly, and the CRCBs experienced an unrecoverable deformation, and the AE ring counts and energy grew by leaps and bounds.

The drastic development stage of AE event occurred mainly in the post-peak failure stage of stress–strain curve. The fractures in the CRCBs propagated and connected with each other rapidly. At this stage, the AE ring count and energy increased by leaps and bounds again. As the loading continued, the AE ring count and energy reached the peak value, and then the bearing capacity of the CRCBs decreased. Meanwhile, the AE ring counts
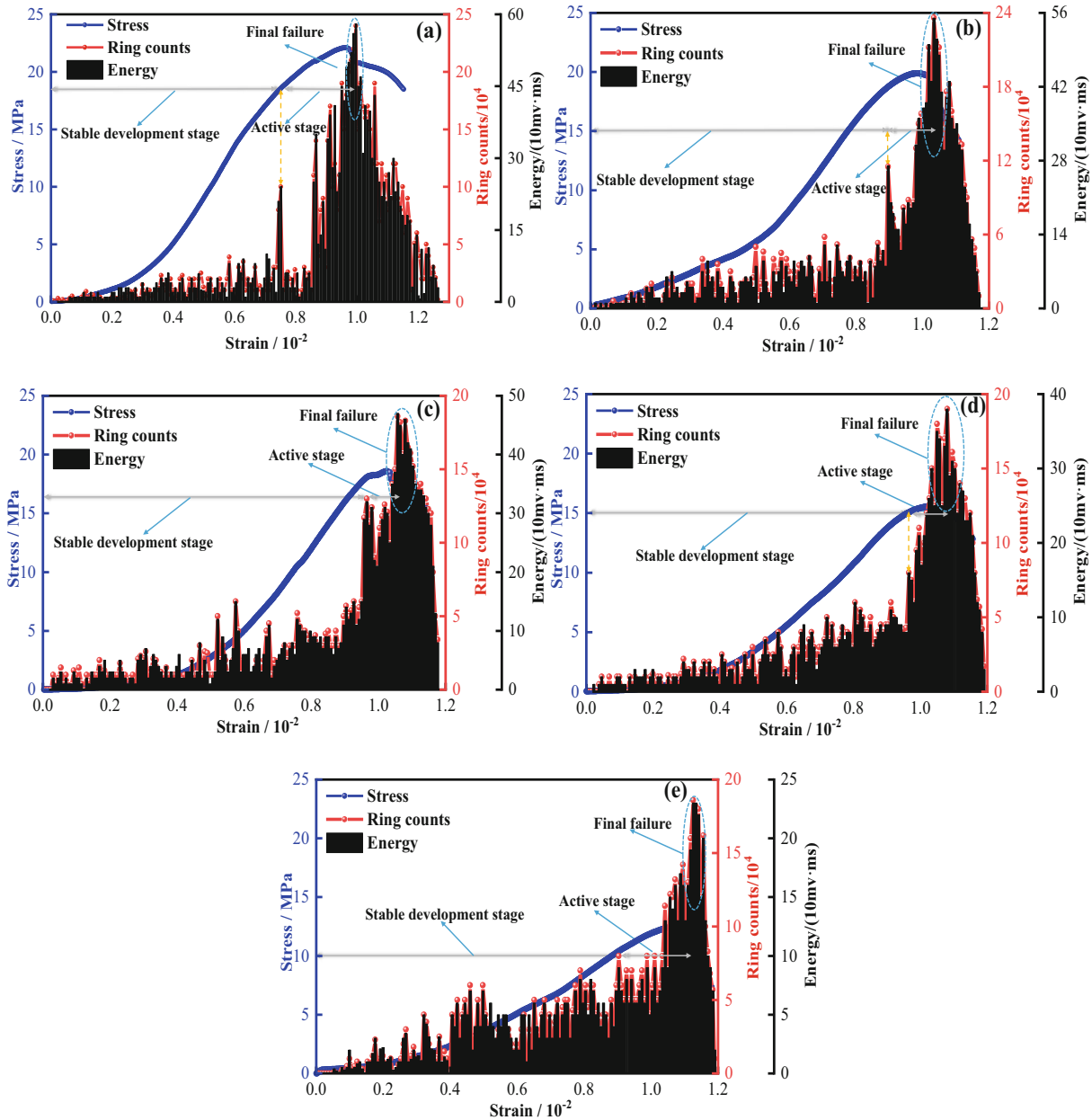
Figure 5. Acoustic emission characteristics of samples of CRCBs with coal thicknesses of (**a**) 10 mm, (**b**) 20 mm, (**c**) 30 mm, (**d**) 40 mm, and (**e**) 50 mm.

and energy began to decrease. The relationship between AE peak ringing counts and peak energy of the CRCBs and the variation of coal thickness is shown in Figures 6 and 7.

It is seen from Figures 6 and 7 that, with increase in coal thickness in the CRCBs, the peak ringing counts and peak energy followed a decreasing trend, but the peak ringing count decreased

slowly and tended eventually to be stable. Because, with increase in coal thickness in the CRCBs, the bearing capacity of the coal part was weaker than that of the rock part, the energy released decreased when the whole CRCBs was broken and the signal value monitored by AE equipment also decreased.
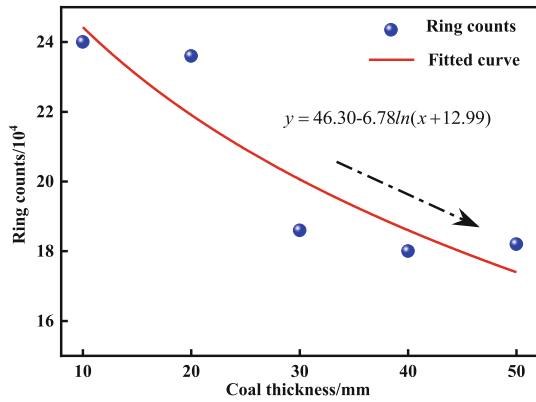
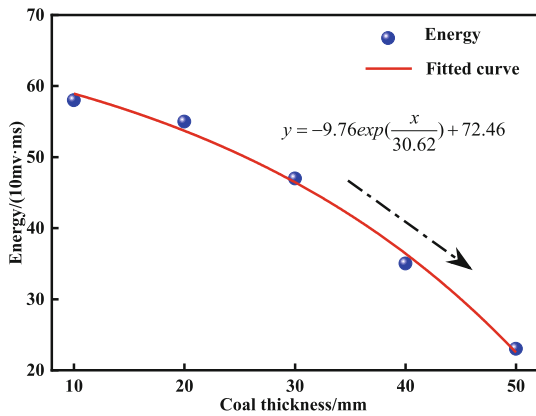**Figure 6.** Variation of peak ring counts with coal thickness.

Figure 8. Energy conversion relationship in sample loading process.

Figure 7. Variation of peak energy with coal thickness.

DISCUSSION

Energy Conversion Characteristics of CRCBs

Dynamic disasters such as rockburst and coal and gas outburst are closely related to the accumulation and release of energy. The induction of external factors will cause the sudden release of energy accumulated in rock mass and coal mass, resulting in catastrophic disasters. Therefore, it is of great significance to master the energy conversion characteristics of coal and rock mass (Xie et al., 2008). Continuous axial stress provides energy to the CRCBs. The conversion of the energy includes mainly two parts: one part is converted into elastic energy and stored in the CRCBs, and the other part is dissipated for supporting the fractures and defects propagation within CRCBs. Suppose there is no heat
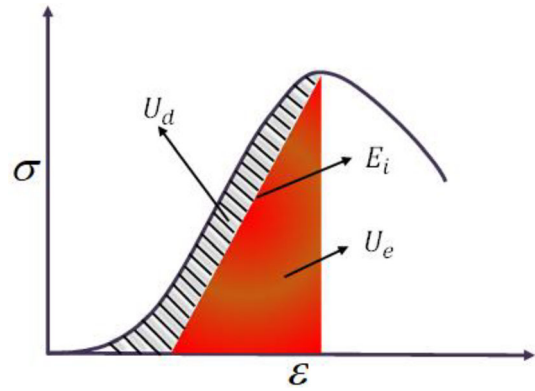
exchange between the samples and the outside environment during the test, then, according to the first law of thermodynamics, the characteristic curve of energy distribution is shown in Figure 8.

The energy conversion characteristics of CRCBs can be expressed as:

$$U = U_e + U_d \qquad (3)$$

where U is the total energy (kJ/m^3) generated by loading, U_e is the elastic energy (kJ/m^3) stored in a sample, and U_d is the energy (kJ/m^3) dissipated to support samples failure. The unit energy relationships in the CRCBs are as follows (Xie et al., 2005):

$$U = \int_0^{\varepsilon_1} \sigma_1 d\varepsilon_1 + \int_0^{\varepsilon_2} \sigma_2 d\varepsilon_2 + \int_0^{\varepsilon_3} \sigma_3 d\varepsilon_3 \qquad (4)$$

$$U^e = \frac{1}{2}\sigma_1\varepsilon_1^e + \frac{1}{2}\sigma_2\varepsilon_2^e + \frac{1}{2}\sigma_3\varepsilon_3^e \qquad (5)$$

where σ_1 is the maximum principal stress (MPa), σ_2 is the intermediate principal stress (MPa), σ_3 is the minimum principal stress (MPa), ε_1, ε_2, and ε_3 are the strains corresponding to σ_1, σ_2, and σ_3, respectively. When $\sigma_2 = 0$ MPa and $\sigma_3 = 0$ MPa under uniaxial compression, the U_e can be expressed according to Hooke's Law, thus:

$$U = \int \sigma_1 d\varepsilon_1 = \sum_1^n \frac{1}{2}(\sigma_{i+1} + \sigma_i)(\varepsilon_{i+1} - \varepsilon_i) \qquad (6)$$

$$U^e = \frac{1}{2E_0}\sigma_1^2 \qquad (7)$$

where E_0 is the initial elastic modulus (the ratio of stress increment and strain increment in the linear stage of stress–strain curve) of the sample during loading.

The energy values of the CRCBs with different coal thicknesses during uniaxial loading were calculated using the above formulas. The energy exchange characteristics of the CRCBs are shown in Figure 9. As shown in Figure 9, the energy conversion characteristics of the CRCBs were classified into four stages according to the changes of elastic energy and dissipated energy of the CRCBs: (1) nonlinear storage stage of elastic energy (OA), (2) linear storage stage of elastic energy (AB), (3) steady growth stage of dissipative energy (BC) and (4) rapid growth stage of dissipation energy (CD).

OA stage. Both the external energy and elastic energy increased exponentially. Part of the energy was dissipated when the initial fractures of CRCBs were closed, and so the dissipated energy increased.

AB stage. Both the total energy and elastic energy rose linearly. Because a small number of fractures was generated inside the CRCBs in this stage, the speed of fractures propagation was relatively slow. Therefore, the dissipated energy remained stable. The external energy was converted mainly into elastic energy and was stored in a sample.

BC stage. The total energy growth trend remained unchanged and the growth rate of elastic energy decreased in this stage. The number of new fractures in the CRCBs increased, the fracture evolution rate increased, and the energy dissipation increased. Therefore, the dissipated energy increased in this stage.

CD stage. This stage was the post-peak stage of the stress–strain curve. The internal fracture evolution rate of CRCBs increased greatly, the bearing capacity decreased, and the external input energy was dissipated mainly by the fractures propagation in the CRCBs. Therefore, the elastic energy decreased greatly and the dissipated energy increased greatly.

Variation Characteristics of Energy Evolution Coefficient of CRCBs

A sample releases its stored elastic energy gradually in the form of local failure under the action of stress concentration in the loading process. In the process of energy dissipation, the local failure of the CRCBs causes the overall failure. The energy dissipation of the sample reflects the degree of failure in the process of loading. Therefore, the failure of the CRCBs under loading can be described by the ratio (k) of dissipated energy (U_d) to elastic strain energy (U_e):

$$k = \frac{U_d}{U_e} \qquad (8)$$

The energy evolution coefficient (k) and the stress–strain curve of CRCBs are shown in Figure 10. As shown in Figure 10, the energy evolution coefficient (k) first grew rapidly and then decreased sharply after the peak in the compaction stage. In this stage, the external energy was consumed due to the closure of the initial fractures inside the CRCBs, and only a small part of the energy was stored in the CRCBs in the form of elastic energy, and so the k was large. In the elastic stage, the decreasing rate of k decreased sharply and finally stabilized and approached to 0, indicating that elastic energy was the main form of energy conversion in this stage. In the plastic stage, k began to rise, and the dissipated energy increased significantly. As the loading continued, the bearing capacity of the CRCBs decreased, and the elastic energy stored in the CRCBs began to release, which eventually led to the CRCBs failure.

The bearing capacity of the CRCBs reached its limit at the stress peak, and then the dissipated energy rose rapidly, making the bearing capacity of the CRCBs continue to decrease until the CRCBs were broken. Therefore, peak stress was not only the turning point of the bearing capacity of the CRCBs, but also the turning point of the growth degree of dissipated energy of the CRCBs. The relationship between k corresponding to peak stress of CRCBs and coal thickness is shown in Figure 11.

Figure 11 shows that the energy evolution coefficient (k) of a sample at the stress peak point decreased linearly as the coal thickness increased in the CRCBs. This means that, with increase in the proportion of coal in the CRCBs, the proportion of elastic energy at the stress peak will increase slightly and the proportion of dissipated energy will decrease. The reason for this phenomenon is that, in the loading process of CRCBs, the rock part is sampled/selected from the rocks in the roof and floor, whose strength is slightly higher than that of coal. When the proportion of the coal part of CRCBs is relatively small, the coal part is destroyed prior to other parts, which leads to the failure of the
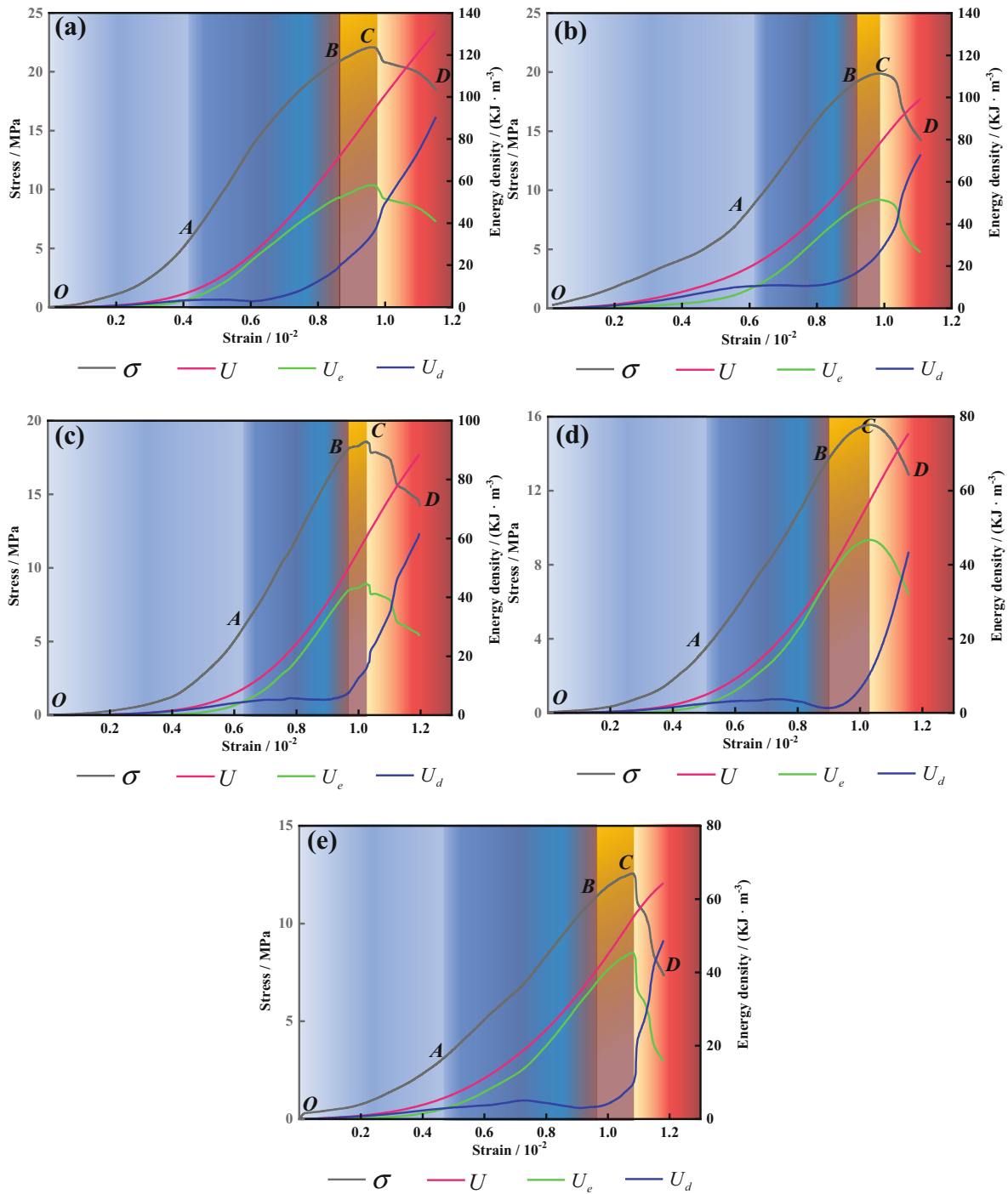
Figure 9. Energy conversion characteristics of the CRCBs at different stress stages when coal thickness was (**a**) 10 mm, (**b**) 20 mm, (**c**) 30 mm, (**d**) 40 mm, and (**e**) 50 mm.

roof and floor rock parts. With increase in coal thickness in the CRCBs, the failure degree of rock part decreases. When the coal thickness reached

50 mm, the rock parts of the CRCBs have no significant failure characteristics. In the process of CRCBs failure, because the hardness of the rock
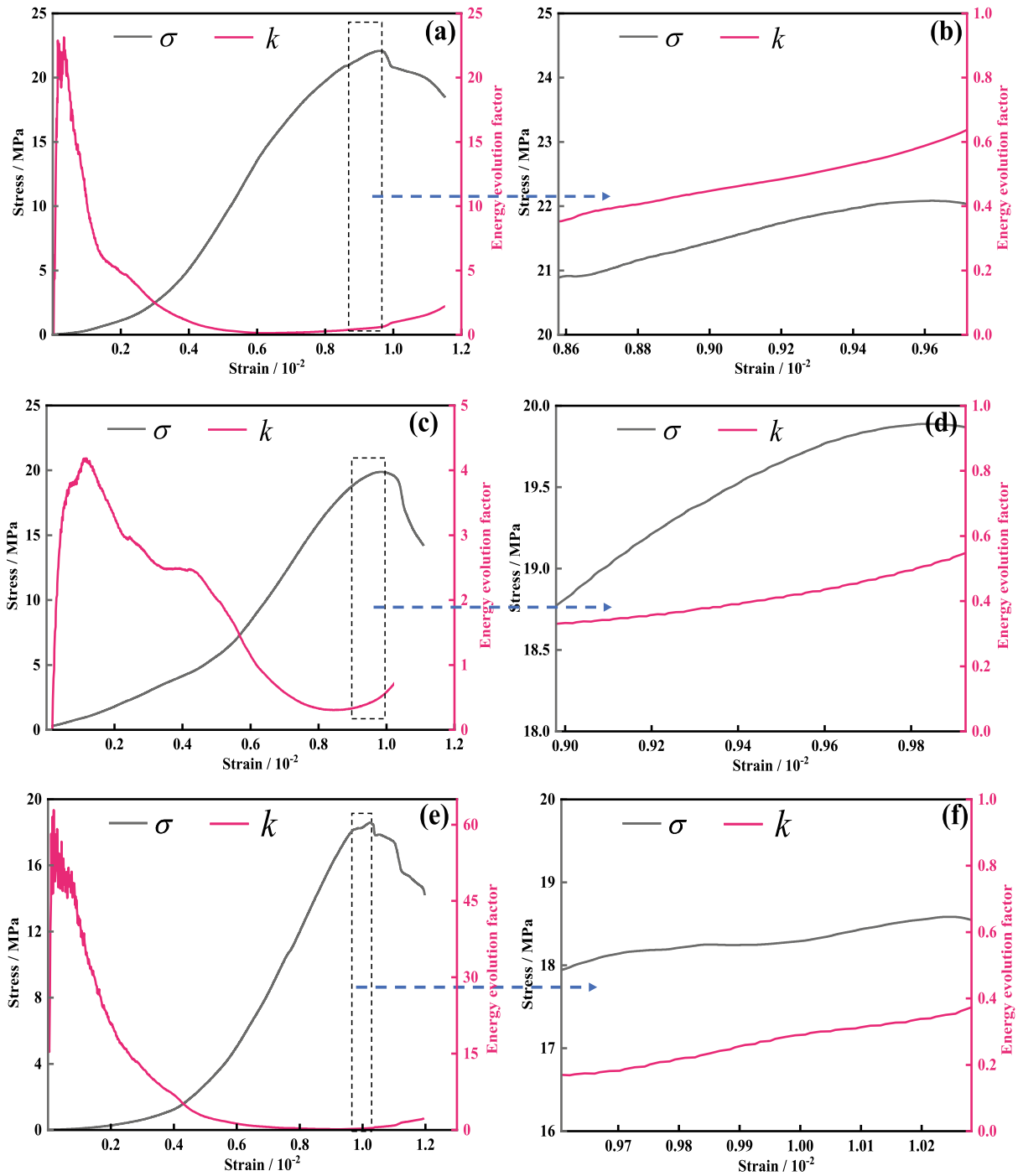
Figure 10. Variation of energy evolution coefficient of CRCBs in different stress stages when coal thickness was: (**a**, **b**) 10 mm; (**c**, **d**) 20 mm; (**e**, **f**) 30 mm; (**g**, **h**) 40 mm; and (**i**, **j**) 50 mm.

part is greater than that of the coal part, and the number of initial fractures in the rock part is less than that in the coal part, the energy consumed in

the failure process is more in the rock part than in the coal part. This indicates that when the coal thickness in the CRCBs increases, the dissipation
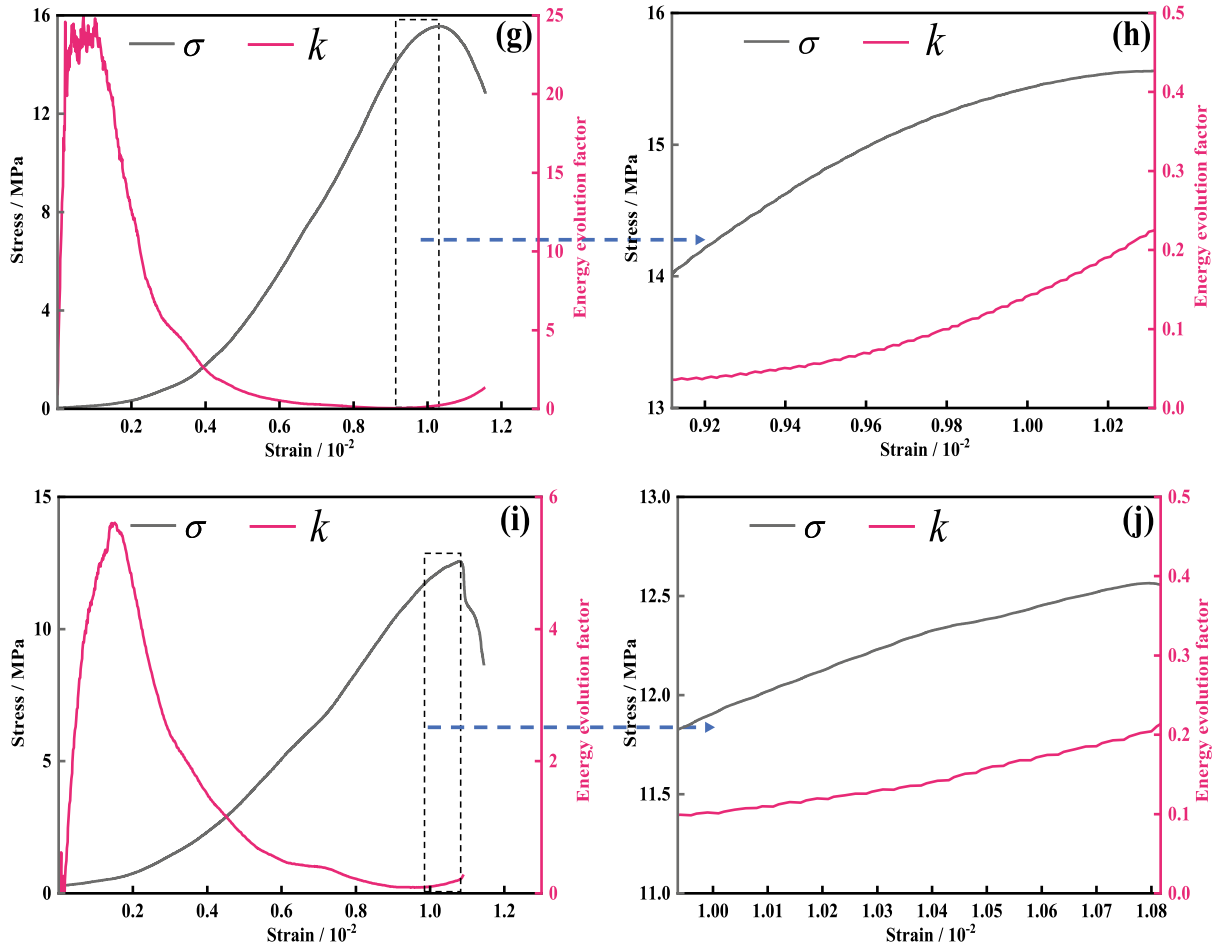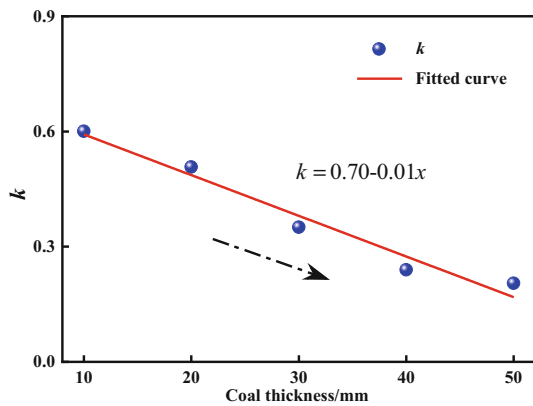
Figure 10. continued.

Figure 11. Relationship between k corresponding to peak stress of CRCBs and coal thickness.

energy used for failure of the rock part decreases greatly, making the overall dissipation energy proportion of the CRCBs decrease.

Energy Storage Limit Analysis of CRCBs

During the construction of large underground projects such as mining engineering and tunnel engineering, the coal and rock mass are affected by the excavation effect, resulting in stress concentration phenomenon. The concentrated stress makes the energy accumulated continuously in coal and rock mass. When the accumulated energy exceeds the storage limit of coal and rock mass, the elastic energy stored in the coal rock will be released instantly, resulting in dynamic disasters, such as rockburst and coal and gas outburst. Therefore, it is

necessary to study the storage energy limit of the CRCBs (Xue et al., 2021a, 2021b). The storage energy limit can be calculated as:

$$U_e^l = \frac{1}{2E_0}\left[\sigma_1^2 + \sigma_2^2 + \sigma_3^2 - 2\mu(\sigma_1\sigma_2 + \sigma_2\sigma_3 + \sigma_1\sigma_3)\right]$$
(9)

Under uniaxial loading, the above equation can be simplified as:

$$U_e^l = \frac{1}{2E_0}\sigma_c^2$$
(10)

where U_e^l is the elastic energy (kJ/m^3) stored in sample when a sample reaches the ultimate compressive strength, and σ_c is the ultimate compressive strength (MPa) of a sample. The variation characteristics of ultimate stored energy of the five samples of CRCBs during uniaxial loading are shown in Figure 12.

It is shown in Figure 12 that, with increase in coal thickness in the CRCBs, the limit energy storage value of the samples decreased logarithmically. The greater the proportion of coal thickness is, the smaller the ultimate energy storage value of the sample is. During the test, it was easier to reach the limit value due to the accumulation of energy, resulting in the failure of a sample. The reason for this phenomenon is the failure of the whole CRCBs was sufficient when the proportion of coal part decreased. With increase in proportion of the coal part, the failure of the CRCBs occurred mainly in the coal part, and the failure of the rock part was not significant. Meanwhile, as the proportion of the coal part of CRCBs increased, the bearing capacity of the whole CRCBs decreased and the energy storage limit of the CRCBs decreased.

Discussion and Analysis of Disaster Reduction by Energy Slow Release

The underground rock mass is usually in the complex and intense gravity stress and tectonic stress field. The coal seam or rock stratum in a coal–rock system deforms under the action of mine pressure and produces elastic strain energy in the system. For the CRCBs in the test, the stresses acting on the coal part and the rock part of CRCBs are equal under load conditions, but the strain of the coal part is larger than that of the rock part due to the difference in elastic modulus of coal and rock. Therefore, under the same stress, more energy is accumulated in the coal part. In engineering practice, if the mine pressure of coal and rock strata is regarded as equal, it is easier for energy to accumulate in the coal seam than in the rock strata. With increase in mining depth, high-energy-level disaster becomes more and more serious, and the high-energy-level dynamic disaster is greatly affected by the lithology of the roof and floor, and the thickness ratio of coal strata. The main inducing factor of high-energy-level dynamic disasters is energy release. Therefore, research on the accumulation law of energy in a coal–rock system plays a key role in the prevention and control of dynamic disaster. In engineering practice, energy in a coal–rock system is accumulated mainly in the coal seam, which is the key energy layer causing dynamic disaster. Less energy accumulated in the rock layer of roof and their main role is clamping coal seam. Coal seam can accumulate more energy under the clamping action of roof and floor. Therefore, the energy accumulation in coal seam is inseparable from the clamping of coal seam by roof and floor. With increase in mining depth, the clamping effect of the roof and floor on the coal seam becomes more significant, which prevents the deformation of the coal seam greatly and makes it difficult to timely release the elastic energy accumulated in it, thus forming the potential safety hazards (Zuo et al., 2018; Zhao et al., 2019; Pan et al., 2020).

In addition, with continuous increase in mining depth, the high in situ stress phenomenon becomes more and more significant, and roof strata, coal seam and floor strata are regarded as conflated, and a complete energy carrier is established. The bearing
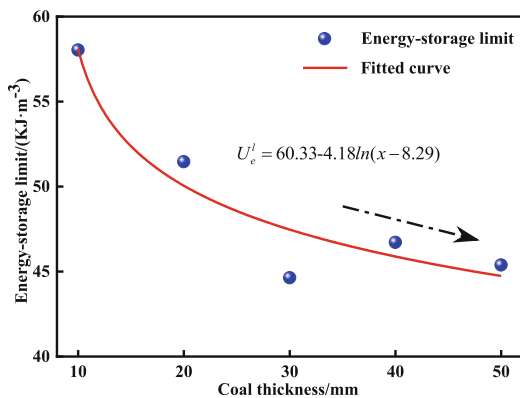

Figure 12. Relationship between storage energy limit and coal thickness of CRCBs.

capacity of the coal seam is relatively weak, and so it is the main structure of energy storage in coal rock system. The coal–rock system is composed of a variety of coal seams with different thicknesses and rock strata with different lithology. Under the action of mine pressure, a lot of energy is accumulated in coal seam, which plays an inducing factor in the overall failure process of coal rock system. Therefore, the coal seam is perceived as the ''key layer of energy accumulation'' in a coal–rock system. So, starting with the energy carrier, slow release of the accumulated energy in the key layer of energy accumulation is fundamental for preventing high-energy-level dynamic disasters. A schematic diagram of energy accumulation position in coal rock system is shown in Figure 13.

In view of this energy carrier structure, the energy accumulated in the key layer of energy accumulation should be released directly, and the energy of roof and floor rocks should be released indirectly, so as to achieve the purpose of preventing and controlling dynamic disasters. Direct release of energy refers to the direct release of energy accumulated in a coal–rock system by changing the physical properties or occurrence characteristics of a coal seam, such as loosening blasting, coal seam infusion and pressure relief by borehole drilling. Indirect release of energy means taking some measures to weaken the clamping effect of the roof or floor of a coal seam to release indirectly the energy accumulated in coal, such as roof blasting and slotting roof (Chen et al., 2020). The essence of these two ways of energy release is to release the energy accumulated in the energy carrier structure by destroying it. In engineering practice, the two measures can be combined to prevent dynamic disasters, and guarantee safety production.
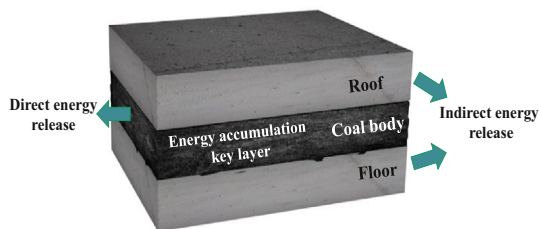

Figure 13. Schematic diagram of energy accumulation position in a coal–rock system.

CONCLUSIONS

This paper treated the coal seam, roof and floor as conflated, and the uniaxial loading test of coal rock composite samples was carried out with the help of MTS uniaxial loading instrument and DS5 AE instrument, and the experimental data of five samples of CRCBs with different coal thicknesses were obtained. According to the law of energy conservation, the failure process of the CRCBs was analyzed from the perspective of energy conversion to support the study of high-energy-level dynamic disasters. The following conclusions were drawn.

1. Because the increase of coal thickness leads to the decrease of the overall carrying capacity of CRCBs, the uniaxial compressive strength and elastic modulus of the CRCBs decrease linearly with increase in coal thickness, while the peak strain shows a linear increasing trend.

2. The variation relationship between AE ring counts and energy is related closely to the failure process of the CRCBs. The variation characteristics of AE events in the failure process of the CRCBs were classified into three stages: (a) stable development stage, (b) active stage, and (c) drastic development stage. With in increase in coal thickness in CRCBs, the overall bearing capacity of a sample decreases, resulting in a trend of decrease in AE peak ringing count and peak energy.

3. In the compaction stage of stress–strain curve, the energy evolution coefficient first grew rapidly and then decreased sharply in the compaction stage. In this stage, the external energy was dissipated to the closure of the initial fractures inside the CRCBs. In the elastic stage, the decreasing rate of the k value decreased sharply, the elastic energy was the main form of energy conversion in this stage. In the plastic stage, k began to rise, and the dissipated energy increased significantly. As the loading continued, the bearing capacity of the CRCBs decreased, and the elastic energy stored in the CRCBs began to release, which eventually led to the CRCBs' failure.

4. With increase in coal thickness in the CRCBs, the limit energy storage value of a sample decreased logarithmically. This shows that the greater the proportion of coal thickness is, the smaller the energy storage limit of the CRCBs is, and the CRCBs are damaged easily.

5. Coal is the main energy storage structure of the whole coal–rock composite system by analyzing the energy accumulation mechanism of coal and rock composite structure in practical engineering. Therefore, we should release artificially the internal energy storage of coal seam and weaken the clamping effect of roof and floor on coal body to change this energy carrier of "roof rock-coal seam-floor rock" structure, so as to achieve the prevention and control of underground dynamic disaster in practical engineering.

ACKNOWLEDGMENTS

DECLARATIONS

CONFLICT OF INTEREST The authors report no declarations of interest.

REFERENCES

Brauner, G. (1975). kritische spannungen in kohleflözen. *Gluck-auf*.

Cao, W., Lin, X., Zhang, C., & Yang, S. (2017). A statistical damage simulation method of dynamic deformation process for rocks based on nonlinear dynamic strength criterion. *Yanshilixue Yu Gongcheng Xuebao/chinese Journal of Rock Mechanics and Engineering, 36*(4), 794–802.

Chen, F., Cao, A., Liang, Z., & Liu, Y. (2021). A coal burst risk assessment model of seismic events based on multiple seismic source parameters: A case study of the huating coal mine, Gansu Province, China. *Natural Resources Research, 30*(6), 4515–4532.

Chen, G., He, M., & Fan, F. (2018). Rock burst analysis using DDA numerical simulation. *International Journal of Geomechanics, 18*(3), 04018001.

Chen, G. B., Li, T., Zhang, G. H., Lv, P. F., & Wu, X. Y. (2020). Experimental study on the law of energy accumulation before failure of coal–rock combined body. *Journal of China Coal Society*. https://doi.org/10.13225/j.cnki.jccs.2020.1511.

Chen, S., Qiao, C. S., Ye, Q., & Deng, B. (2018). Composite damage constitutive model of rock mass with intermittent joints based on Mohr-Coulomb criterion. *Yantu Lixue/rock and Soil Mechanics, 39*(10), 3612–3622.

Chen, Z., He, C., Ma, G., Xu, G., & Ma, C. (2019). Energy damage evolution mechanism of rock and its application to brittleness evaluation. *Rock Mechanics and Rock Engineering, 52*(4), 1265–1274.

Cook, N., Hock, E., Pretorius, J. P. G, Ortlepp, W. D, & Salamon, M. D. (1966). Rock mechanics applied to study of rockbursts. *Journal of South African Institute of Mining and Metallurgy*, 435–528.

Cook, N. G. W. (1963). The basic mechanics of rockbursts. *Journal of the South African Institute of Mining and Metallurgy, 64*, 71–81.

Cook, N. G. W. (1965). A note on rockbursts considered as a problem of stability. *Journal of the South African Institute of Mining and Metallurgy, 65*, 551–554.

Deist, F. H. (1965). A nonlinear continuum approach to the problem of fracture zones and rockbursts. *Journal- South African Institute of Mining and Metallurgy, 65*(10), 502–522.

Dong, L., Chen, Y., Sun, D., & Zhang, Y. (2021). Implications for rock instability precursors and principal stress direction from rock acoustic experiments. *International Journal of Mining Science and Technology, 31*(5), 789–798.

He, Y., Zhao, P., Li, S., Ho, C. H., Zhu, S., Kong, X., & Barbieri, D. M. (2021). Mechanical properties and energy dissipation characteristics of coal–rock-like composite materials subjected to different rock-coal strength ratios. *Natural Resources Research, 30*(3), 2179–2193.

Hong, T., Zhang, D., Wang, W., & Cai, M. (2021). Acoustic emission characteristics of high-strength self-compacting recycled lump concrete under uniaxial compression. *Journal of Huaqiao University (natural Science), 42*(3), 351–357.

Huang, B., & Liu, J. (2013). The effect of loading rate on the behavior of samples composed of coal and rock. *International Journal of Rock Mechanics and Mining Sciences, 61*, 23–30.

Jiang, J., Wang, P., Jiang, L., Zheng, P., & Feng, F. (2018). Numerical simulation on mining effect influenced by a normal fault and its induced effect on rock burst. *Geomechanics and Engineering, 14*(4), 337–344.

Lemaitre, J. (1984). How to use damage mechanics. *Nuclear Engineering and Design, 80*(2), 233–245.

Li, H., Shen, R., Qiao, Y., & He, M. (2021). Acoustic emission signal characteristics and its critical slowing down phenomenon during the loading process of water-bearing sandstone. *Journal of Applied Geophysics, 194*, 104458.

Li, H. C., & Zhang, S. (2017). A constitutive damage model of rock based on the assumption of modified Lemaitre strain equivalence hypothesis. *Yantu Lixue/rock and Soil Mechanics, 38*(5), 1321–1334.

Li, S., Zhao, B., Lin, H., Shuang, H., Kong, X., & Yang, E. (2021). Review and prospects of surfactant-enhanced spray dust suppression: Mechanisms and effectiveness. *Process Safety and Environmental Protection, 154*, 410–424.

Li, X. L., Cao, Z. Y., & Xu, Y. L. (2020). Characteristics and trends of coal mine safety development, energy sources. *Part a: Recovery, Utilization, and Environmental Effects, 12*, 1–19.

Li, X. L., Chen, S. J., Li, Z. H., & Wang, E. Y. (2021a). Rockburst mechanism in coal rock with structural surface and the microseismic (MS) and electromagnetic radiation (EMR) response. *Engineering Failure Analysis, 124*(3), 105396.

Li, X. L., Chen, S. J., Liu, S. M., & Li, Z. H. (2021c). AE waveform characteristics of rock mass under uniaxial loading based on Hilbert–Huang transform. *Journal of Central South University, 28*(6), 1843–1856.

Li, X. L., Chen, S. J., Zhang, Q. M., Gao, X., & Feng, F. (2021b). Research on theory, simulation and measurement of stress behavior under regenerated roof condition. *Geomechanics and Engineering, 26*(1), 49–61.

Liu, A., & Liu, S. (2021). A fully-coupled water-vapor flow and rock deformation/damage model for shale and coal: its application for mine stability evaluation. *International Journal of Rock Mechanics and Mining Sciences, 146*(12), 104880.

Liu, Y., & Dai, F. (2018). A damage constitutive model for intermittent jointed rocks under cyclic uniaxial compression. *International Journal of Rock Mechanics and Mining Sciences, 103*, 289–301.

Liu, S. M., Li, X. L., Wang, D. K., & Zhang, D. M. (2020). Experimental study on temperature response of different

ranks of coal to liquid nitrogen soaking. *Natural Resources Research., 32*(2), 1467–1480.

Liu, W., Qian, D., Yang, X., Wang, S., Deng, J., Cui, Q., & Li, Z. (2021). Stress relief and support for stability of deep mining roadway with thick top coal in Hujiahe coal mine with the risk of rock burst. *Shock and Vibration, 2021*, 3822336.

Liu, Y., Sun, H., Wang, B., Dai, L., & Cao, J. (2021). Experimental accuracy and stability of gas outburst experimental system. *Geofluids, 2021*(4), 6678608.

Lu, H., Zhang, R., Ren, L., Zhang, A., Yang, Y., & Li, X. (2021). *Damage Characterization of Shale under Uniaxial Compression by Acoustic Emission Monitoring, 15*, 817–830.

Ma, Q., Tan, Y. L., Liu, X. S., Zhao, Z. H., & Fan, D. Y. (2021). Mechanical and energy characteristics of coal–rock composite sample with different height ratios: A numerical study based on particle flow code. *Environmental Earth Sciences, 80*(8), 1–14.

Maleki, H. (2021). High stress gradient, critical factor affecting rock burst in the United States mines. *IOP Conference Series: Earth and Environmental Science, 833*(1), 012122.

Meng, Q., Zhang, M., Zhang, Z., Han, L., & Pu, H. (2018). Experimental research on rock energy evolution under uniaxial cyclic loading and unloading compression. *Geotechnical Testing Journal, 41*(4), 717–729.

Miao, S., Pan, P. Z., Konicek, P., Yu, P., & Liu, K. (2021). Rock damage and fracturing induced by high static stress and slightly dynamic disturbance with acoustic emission and digital image correlation techniques. *Journal of Rock Mechanics and Geotechnical Engineering, 13*(5), 1002–1019.

Mroz, Z., & Nawrocki, P. (1989). Deformation and stability of an elasto-plastic softening pillar. *Rock Mechanics and Rock Engineering, 22*(2), 69–108.

Niu, X. (2018). Impact analysis of the open type crack characteristics of coal and rock burst. *IOP Conference Series: Earth and Environmental Science, 208*(1), 012031.

Pan, Y., Li, Z., & Zhang, M. (2003). *Distribution, type, mechanism and prevention of rockbrust in China*.

Pan, J. F., Liu, S. H., Gao, J. M., Sun, X. K., Xia, Y. X., & Wang, Q. (2020). Prevention theory and technology of rock burst with distinguish dynamic and static load sources in deep mine roadway. *Journal of China Coal Society, 45*(5), 1607–1613.

Pang, M. K., Zhang, T. J., Gao, L., & Qin, B. F. (2021). Investigating the effects of effective stress on pore-dependent permeability measurements of crushed coal. *PLoS ONE, 16*(12), e0261678.

Qi, Q., Shi, Y., & Liu, T. (1997). Mechanism of instability caused by viscous sliding in rock burst. *Journal of China Coal Society, 22*(2), 144–148.

Salamon, M. (1964a). Elastic analysis of displacement and stress induced by the mining of seam or reef deposits—Part I. *Journal of South African Institute of Mining and Metallurgy*, 197–218.

Salamon, M. (1964b). Elastic analysis of displacement and stress induced by the mining of seanl or reef deposits—Part II. *Journal of South African Institute of Mining and Metallurgy*, 129–149.

Salamon, M. (1964c). Elastic analysis of displacement and stress induced by the mining of seanl or reef deposits—Part III. *Journal of South African Institute of Mining and Metallurgy*, 468–500.

Schiavi, A., Niccolini, G., Tarizzo, P., Carpinteri, A., Lacidogna, G., & Manuello, A. (2011). Acoustic emissions at high and low frequencies during compression tests in brittle materials. *Strain, 47*, 105–110.

Shi, X. Q., Chen, X. K., Zhang, Y. T., Zhang, Y. B., Guo, R. Z., Zhao, T. L., & Liu, R. (2022). Numerical simulation of coal dust self–ignition and combustion under inclination conditions. *Energy, 239*(1), 122227.

Shi, X. Q., Zhang, Y. T., Chen, X. K., & Zhang, Y. B. (2021). Effects of thermal boundary conditions on spontaneous combustion of coal under temperature-programmed conditions. *Fuel, 295*, 120591.

Sun, H., Dai, L., Liu, Y., & Jin, H. (2021). Critical conditions and energy transfer characteristics of the failure process of coal–rock combination systems in deep mines. *Geofluids, 2021*(16), 6655443.

Wang, Y. (2021). Prediction of rockburst risk in coal mines based on a locally weighted c4.5 algorithm. *IEEE Access, 9*, 15149–15155.

Wang, G., & Huang, G. (2012). Areview on rockburst theories. *China Mining Magazine, 21*, 400–405.

Wang, L., Cao, A., Dou, L., Guo, W., Zhang, Z., Zhi, S., & Zhao, Y. X. (2019). Numerical simulation on failure effect of mining-induced dynamic loading and its influential factors. *Safety Science, 113*, 372–381.

Wang, P., Jiang, L. S., Zheng, P. Q., Qin, G. P., & Zhang, C. (2019). Inducing mode analysis of rock burst in fault-affected zone with a hard–thick stratum occurrence. *Environmental Earth Sciences, 78*(15), 1–13.

Wang, Z. L., Shi, H., & Wang, J. G. (2018). Mechanical behavior and damage constitutive model of granite under coupling of temperature and dynamic loading. *Rock Mechanics and Rock Engineering, 51*(10), 3045–3059.

Xie, H., Ju, Y., & Li, L. (2005). Criteria for strength and structural failure of rocks based on energy dissipation and energy release principles. *Chinese Journal of Rock Mechanics and Engineering, 24*(17), 3003–3010.

Xie, H., Ju, Y., Li, L., & Peng, R. (2008). Energy mechanism of deformation and failure of rock masses. *Chinese Journal of Rock Mechanics and Engineering, 27*(9), 1729–1740.

Xu, J., Cheng, L., Zhou, B., Peng, S., Yang, X., & Yang, W. (2021). Experimental study of gas concentration and its thermal behavior in coal and gas outburst. *Arabian Journal of Geosciences, 14*(18), 1–10.

Xue, D., Lu, L., Gao, L., Lu, L., & Chen, C. (2021). Prediction of fracture and dilatancy in granite using acoustic emission signal cloud. *Journal of Rock Mechanics and Geotechnical Engineering, 13*(5), 1059–1077.

Xue, J., Du, X., Ma, Q., & Zhan, K. (2021). Experimental study on law of limit storage energy of rock under different confining pressures. *Arabian Journal of Geosciences, 14*(1), 62.

Yang, Y., & Zhang, Z. (2021). Surrounding rock effect on coal burst under unloading condition: A numerical study. *Arabian Journal of Geosciences, 14*, 1742.

Yang, Q. L., Li, W., & Jin, K. (2020). Supercritical CO_2 interaction induced pore morphology alterations of various ranked coals: A comparative analysis using corrected mercury intrusion porosimetry and low-pressure N_2 gas adsorption. *ACS Omega, 5*(16), 9276–9290.

Yang, Q. L., Xue, J. H., Li, W., Hu, B., Du, X. H., Ma, Q., Zhan, K. L., & Chen, Z. H. (2021a). Comprehensive evaluation and interpretation of mercury intrusion porosimetry data of coals based on fractal theory. *Tait Equation and Matrix Compressibility. Fuel, 298*, 120823.

Yang, Q. L., Xue, J. H., Li, W., Hu, B., Ma, Q., Zhan, K. L., Du, X. H., & Chen, Z. H. (2021b). Reconstructions of supercritical CO_2 adsorption isotherms and absolute adsorption estimation in nanoporous coals considering volumetric effects and varying adsorbed phase densities. *Chemical Engineering Journal, 433*(part 2), 133492.

Yang, Z., Liu, C., Zhu, H., Xie, F., Dou, L., & Chen, J. (2019). Mechanism of rock burst caused by fracture of key strata during irregular working face mining and its prevention methods. *International Journal of Mining Science and Technology, 29*(6), 889–897.

Yin, T., Wang, P., Yang, J., & Li, X. (2018). Mechanical behaviors and damage constitutive model of thermally treated sandstone under impact loading. *IEEE Access, 6*, 72047–72062.

Yu, W. J., Pan, B., Li, K., & Shen, W. B. (2021). Mechanical properties and fracture evolution law of rock-coal–rock combination. *Journal of China Coal Society*. https://doi.org/10.13225/j.cnki.jccs.XR21.1563.

Yu, Z., Wen, J., Ma, H., & Wei, Q. (2021). Research on the evolution law of spatial structure of overlying strata and evaluation of rock burst risks in deep well strip mining. *Geotechnical and Geological Engineering, 39*(7), 5095–5107.

Zhang, M. (1987). Instability theory and mathematical model for coal/rock bursts. *Chinese Journal Rock Mechanics and Engineering, 3*, 197–204.

Zhang, W., Ma, N., Ma, J., Li, C., & Ren, J. (2020). Mechanism of rock burst revealed by numerical simulation and energy calculation. *Shock and Vibration, 2020*, 8862849.

Zhang, Y., Li, B., Xu, J., Gao, Z., Chen, S., & Wang, B. (2021). Study on triaxial compression damage evolution characteristics of coal based on energy dissipation. *Chinese Journal of Rock Mechanics and Engineering, 40*(8), 1614–1627.

Zhang, Z., Xie, H., Zhang, R., Zhang, Z., Gao, M., Jia, Z., & Xie, J. (2019). Deformation damage and energy evolution characteristics of coal at different depths. *Rock Mechanics and Rock Engineering, 52*(5), 1491–1503.

Zhao, B., Li, S. G., Lin, H. F., Cheng, Y. Y., Kong, X. G., & Ding, Y. (2022). Experimental study on the influence of surfactants in compound solution on the wetting-agglomeration properties of bituminous coal dust. *Powder Technology, 395*, 766–775.

Zhao, K., Yang, D. X., Zeng, P., Ding, J. H., Gong, C., Wang, X. J., & Zhong, W. (2020). Frequency-domain characteristics of acoustic signals of granite under uniaxial compression. *Chinese Journal of Geotechnical Engineering, 42*(12), 2189–2197.

Zhao, S. K., Deng, Z. G., Ji, W. B., Li, Z. G., Zhang, G. H., & Li, Y. Z. (2019). Effects of multi-stage tectonic movement on regional tectonic stress characteristics and rockburst. *Journal of Mining and Safety Engineering, 36*(2), 306–314.

Zhao, Y., Gong, S., Hao, X., Peng, Y., & Jiang, Y. (2017). Effects of loading rate and bedding on the dynamic fracture toughness of coal: Laboratory experiments. *Engineering Fracture Mechanics, 178*, 375–391.

Zhou, T., Qin, Y., Ma, Q., & Liu, J. (2019). A constitutive model for rock based on energy dissipation and transformation principles. *Arabian Journal of Geosciences, 12*(15), 1–14.

Zhou, X., & Zhang, J. (2021). Damage progression and acoustic emission in brittle failure of granite and sandstone. *International Journal of Rock Mechanics and Mining Sciences, 143*, 104789.

Zhu, G. A., Dou, L. M., Wang, C. B., Li, J., Cai, W., & Ding, Z. W. (2017). Numerical investigation of the evolution of overlying strata and distribution of static and dynamic loads in a deep island coal panel. *Arabian Journal of Geosciences, 10*(24), 1–22.

Zubelewica, O. C., & Mroz, Z. (1983). Numerical simulation of rockburst processes treated as problems of dynamite instability. *Rock Mechanics and Engineering, 16*(4), 253–274.

Zuo, J. P., Chen, Y., & Cui, F. (2018). Investigation on mechanical properties and rock burst tendency of different coal–rock combined bodies. *Journal of China University of Mining and Technology, 47*(1), 81–87.